

An Error Budget for the JPL Hydrogen Maser Receiver

C. A. Greenhall

Communications Systems Research Section

This report estimates the frequency instability and phase noise of the hydrogen maser receiver. The errors at each output are given as functions of the errors of the component modules of the receiver. The results are compared to the measured errors of the frequency standard (maser plus receiver).

I. Introduction

The hydrogen maser receiver is a synthesizer that converts the maser signal, at about 1420 MHz, to a set of output signals at 100, 20, 10, 5, 1, and 0.1 MHz. This report estimates the contribution of the receiver and its component modules to the frequency instability and phase noise of each of its outputs, and compares these results to published measurements of the 100-MHz output of the frequency standard, which consists of a maser plus its receiver. One can then assess how much the receiver degrades the performance of the frequency standard.

The block diagram of the receiver is shown in Fig. 1, which is extracted from Ref. 1 and modified slightly. It is a double-heterodyne phase-locked loop that provides its own mixing signals to the first and second mixers. The frequency conversion ratio of the receiver is tuned by setting the conversion ratio of the synthesizer that feeds one side of the phase detector. Let us believe that the maser is oscillating at $1420 + f_s$ MHz. If the synthesizer's front panel dials are set to read f_s MHz, then the loop forces the receiver outputs to have their advertised frequencies of 0.1 up to 100 MHz, relative to the $1420 + f_s$ MHz that we believe the maser to have. The frequency f_s can be set between 0.4 and 0.51 MHz in steps of 10^{-8} Hz.

In the following analysis, we presume to traverse the territory covered by R. Meyer in Ref. 1. There are a few differences. First, many of the component performances in Ref. 1 are merely requirements. Some of these we have replaced by the measured performances reported in a number of other references, to be cited later. Second, we have given a more thorough treatment of the effect of the distribution amplifier chain on the loop and on the receiver outputs. Finally, we have added one more (somewhat redundant) performance measure, the Allan variance for $\tau = 1$ second, because it is easy to compare it with measurements on the frequency standard.

II. Phase Noise Breakdown

The aim here is to give the phase noises at the six outputs, (13) to (18) in Fig. 1, in terms of the phase noises contributed by the component modules. The sinewave signal at point (i) in the figure has phase noise ϕ_i at the indicated frequency (MHz). An exception is the baseband signal at (5). There are many sources of noise. If a module (call it Z) has one output, then the additive phase noise contributed by Z to its output is called n_Z . If Z has several outputs, at (i), (j), \dots , then there are several noises n_{Zi} , n_{Zj} , \dots blamed on Z . All of the outputs of each distribution amplifier (DA) are electrically

separate, even though the figure shows the noises n_{I20} , n_{I21} , n_{I22} as coming from the same point. Each of the modules H through L is a divider, cleanup filter, and DA in tandem.

The signal at ⑤, the phase detector output, is

$$K_D [A \sin(\phi_4 - \phi_{10} + n_D) + n_t]$$

where K_D is the phase detector gain, and A is the rms amplitude of the signal at ④. The noise n_D is an exception to the above rules in that it is referred to the input of D instead of the output. The term n_t is the baseband equivalent of the thermal noise of the receiver.

The linearized equation of motion of the phase noise ϕ_6 can now be written as

$$[1 + 14.204 G(s)] \phi_6 = G(s)n + n_E$$

where the synthesizer frequency f_s has been set to 0.4 MHz, and

$$G(s) = AK_D K_{VCO} F(s)/s,$$

$$n = n_t/A + n_A + n_B + n_C + n_D - n_M - n_{H11} - n_G - 14n_{F7} - 0.2 n_{F8} - 0.004 n_{F9}.$$

(1)

From now on, let us drop the term $0.004n_{F9}$ and replace 14.204 by 14.2. The closed-loop transfer function is

$$L(s) = \frac{14.2 G(s)}{1 + 14.2 G(s)},$$

whose two-sided noise bandwidth is 100 Hz (Ref. 2). The phase noise ϕ_6 can be written

$$\phi_6 = L(s)(n/14.2) + [1 - L(s)] n_E.$$

(2)

Thus, $n/14.2$ appears inside the loop passband, and n_E appears outside.

The output phase noises, presented as if they were multiplied up to 100 MHz, are

$$100 \text{ MHz: } \phi_{13} = \phi_6 + n_{F13}$$

$$20 \text{ MHz: } 5\phi_{14} = \phi_6 + n_{F8} + 5n_{H14}$$

$$10 \text{ MHz: } 10\phi_{15} = \phi_6 + n_{F19} + 10n_{I15} \quad (3)$$

$$5 \text{ MHz: } 20\phi_{16} = \phi_6 + n_{F19} + 10n_{I20} + 20n_J$$

$$1 \text{ MHz: } 100\phi_{17} = \phi_6 + n_{F19} + 10n_{I21} + 100n_K$$

$$0.1 \text{ MHz: } 1000\phi_{18} = \phi_6 + n_{F19} + 10n_{I22} + 1000n_L$$

III. Phase Noise Data Types

We can now discuss Table 1, which contains most of the results of this report. The first data type is called $\Delta f/f$. It is the maximum change in relative frequency that occurs after the receiver environment undergoes a sudden 5°C change in temperature. The *output* column gives the estimated $\Delta f/f$ for each of the six receiver outputs, 100 MHz down to 0.1 MHz. The *standalone* column gives the $\Delta f/f$ for each component by itself. The *receiver* column gives the modular contributions that must be summed according to the arrows to give $\Delta f/f$ for the six outputs. Since some of the $\Delta f/f$ contributions may have different signs, this is a worst-case result.

To arrive at the receiver $\Delta f/f$ numbers, one has to account not only for the coefficients in Eqs. (1) – (3), but also for the frequencies at different places in the loop. For example, ϕ_6 is at 100 MHz, n_A is at about 1420 MHz, and n_B is at 20.4 MHz. From Eqs. (1) and (2), since $L(0) = 1$,

$$\phi_6 = \frac{1}{14.2} (n_A + n_B) + \text{others},$$

$$\frac{\phi_6}{100} = \frac{n_A}{1420} + \frac{20.4}{1420} \frac{n_B}{20.4} + \text{others}.$$

This shows that

$$\text{receiver } \Delta f/f = \text{standalone } \Delta f/f \quad (\text{module A})$$

$$\text{receiver } \Delta f/f = (20.4/1420) (\text{standalone } \Delta f/f) \quad (\text{module B}).$$

The second data type is one-sided spectral density of phase, $S_{\phi}(f)$, evaluated at $f = 10$ Hz. The units are dB relative to $1 \text{ rad}^2/\text{Hz}$. This gives an idea of the relative sizes of the short-term phase noises. The *receiver and output* S_{ϕ} values are referred to 100 MHz, and the receiver values are summed according to the arrows. For the above example,

$$S_{\phi_6}(f) = \left(\frac{1}{14.2}\right)^2 [S_{n_A}(f) + S_{n_B}(f)] + \text{others}.$$

This shows that the receiver values are $(1/14.2)^2$ (-23 dB) times the standalone values for those two modules. Note that the figure -100 dB for the 0.1-MHz output is the spectral density of $1000\phi_{18}$, not ϕ_{18} , whose spectral density is -160 dB.

The third data type is Allan deviation (square root of Allan variance) at $\tau = 1$ second, computed from the phase noise models used to get $S_\phi(f)$. Each output value is the rss of the receiver values indicated by the arrows.

IV. The Bottom Line

The hydrogen maser is viewed only through the window of its receiver. The last line of Table 1 gives results of measurements made on the 100-MHz output of the combined system (Refs. 3, 4). These can be compared directly to our estimates

of the instability of the receiver alone at its 100-MHz output. The thermal $\Delta f/f$ of the receiver (a worst-case estimate) is 0.52 times the measured system value, the receiver $S_\phi(10)$ is 6 dB below the measured system value, and the receiver $\sigma_y(1)$ is 0.43 times the measured system value.

Figure 2 extends the $\sigma_y(\tau)$ comparison over a wide range of τ . The two upper curves are measurements of Allan deviation (Refs. 3, 5) of hydrogen maser frequency standards at 100 MHz. The lower curve is our estimate of the contribution of the receiver. It is composed mainly of thermal noise from the front end of the receiver and flicker phase modulation from the 100-MHz distribution amplifier. For $\tau < 30$ s the receiver noise is 3 dB to 7 dB below the total system noise. To put it another way, the receiver appears to degrade the short-term stability of the maser by 1 to 3 dB. For larger τ , the degradation from random receiver noise is negligible.

Acknowledgment

I would like to thank Roger Meyer for his patient assistance and the loan of his hydrogen maser bibliography.

Table 1. Frequency instability and phase noise of JPL hydrogen maser receiver

Module	Standalone	$\Delta f/f$ for $S^\circ C$ step Receiver	Output	Standalone MHz	S_ϕ (10 Hz) Referred to 100 MHz Receiver	Output	Receiver σ_y (1 s)	Output
Thermal noise				-84 dB	1420	-107 dB	9E-14	
						↓	↓	
A. Front end	1E-14	1E-14		-124 dB	1420	-147 dB	1E-15	
		↓				↓	↓	
B. First IF	7E-15	1E-16		-124 dB	20.4	-147 dB	1E-15	
		↓				↓	↓	
C. Second IF	3.5E-15	1E-16		-124 dB	0.406	-147 dB	1E-15	
		↓				↓	↓	
D. Phase detector	3.5E-13	1E-16		-124 dB	0.406	-147 dB	1E-15	
		↓				↓	↓	
M. X14	1.8E-13	1.8E-13		-110 dB	1400	-133 dB	5.4E-15	
		↓				↓	↓	
G. Dana synthesizer	3.4E-15	1E-18		-128 dB	0.406	-151 dB	6.6E-16	
		↓				↓	↓	
E. 100 MHz VCO	2E-12	<7E-17		-104 dB	100	<-147 dB	6.6E-15	
		↓				↓	↓	
F. 100 MHz DA	3.7E-14	7.4E-14		-111 dB	100	-108 dB	1E-13	
		↓				↓	↓	
								→ 1.3E-13
H. ÷5, 20 MHz DA	2.4E-13	3.3E-15 → 2.4E-13	→ 5E-13	-121 dB	20	-144 dB → -107 dB → -103 dB	1.5E-15 → 1.1E-13 → 1.7E-13	
		↓				↓	↓	
I. ÷10, 10 MHz DA	2.4E-13	2.4E-13	→ 7.5E-13	-127 dB	10	-107 dB	1.1E-13	→ 2.1E-13
J. ÷2, 5 MHz DA	2.4E-13	→ 2.4E-13	→ 1E-12	-133 dB	5	→ -107 dB → -100 dB	→ 1.1E-13 → 2.3E-13	
K. ÷10, 1 MHz DA	2.4E-13	→ 2.4E-13	→ 1E-12	-147 dB	1	→ -107 dB → -100 dB	→ 1.1E-13 → 2.3E-13	
L. ÷100, 0.1 MHz DA	2.4E-13	→ 2.4E-13	→ 1E-12	-167 dB	0.1	→ -107 dB → -100 dB	→ 1.1E-13 → 2.3E-13	
H maser + receiver, measured at 100 MHz			5E-13			-98 dB		3E-13

Table 2. Breakdown of modules H-L

	$\frac{\Delta f}{f}$ 5°C step $\tau = 2000$ s	$S_{\phi}(10 \text{ Hz})$ $f_0 = 1000 \text{ MHz}$	$\sigma_y(1 \text{ s})$
Frequency divider	1.9E-13	-114 dB	4.8E-14
Cleanup filter	9.3E-15	-111 dB	6.8E-14
Distribution amplifier	3.7E-14	-111 dB	6.8E-14
Total	2.4E-13	-107 dB	1.1E-13
	sum	sum	rss

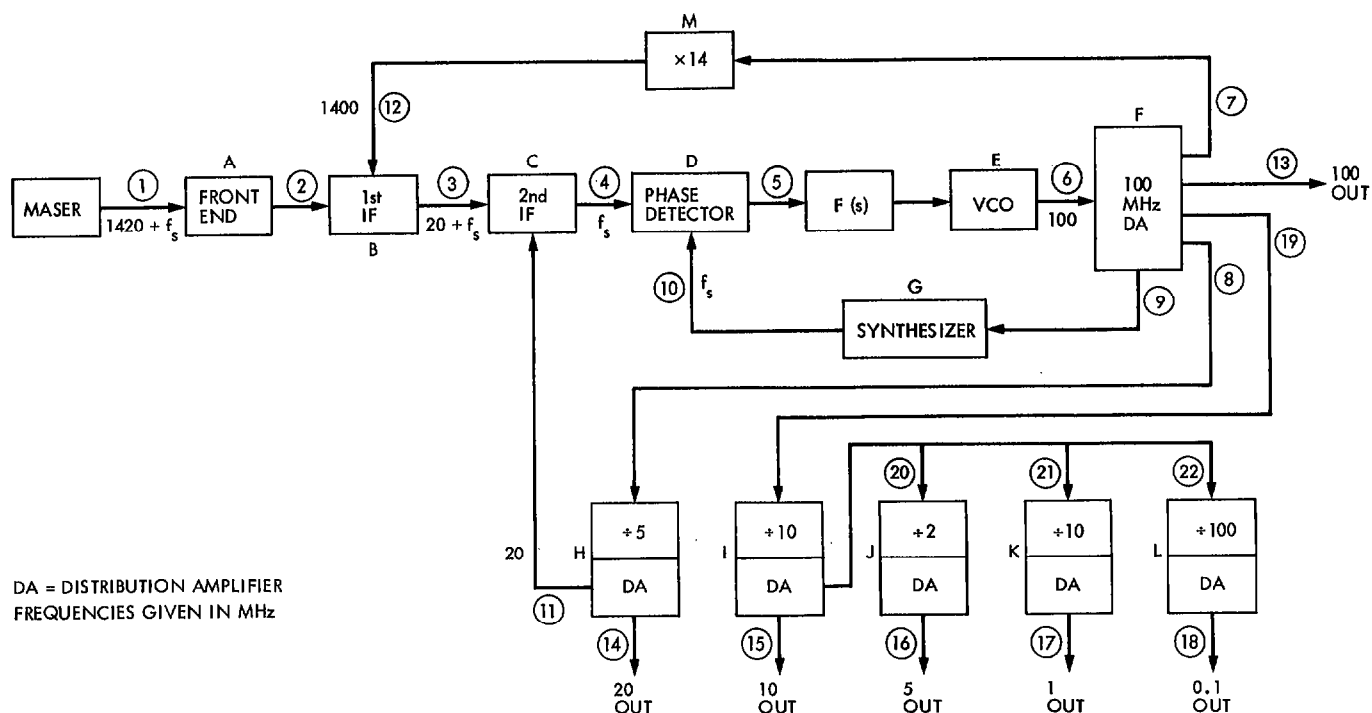


Fig. 1. Hydrogen maser receiver block diagram

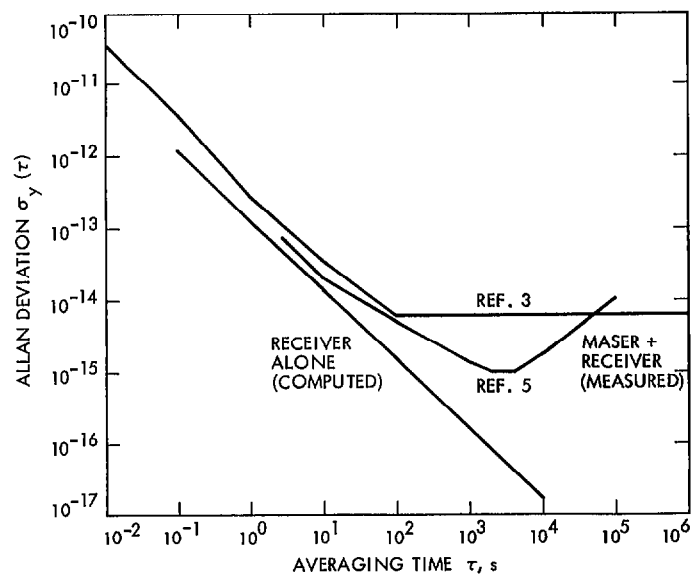


Fig. 2. Frequency stability of hydrogen maser receiver and total system at 100 MHz

Appendix A

Discussion of Receiver Modules

Thermal noise. (This has nothing to do with the $\Delta f/f$ caused by a thermal step.) According to Ref. 2, the receiver loop has SNR $\rho = 64$ dB in $2b_L = 100$ Hz. If N_0 is the one-sided spectral density of the thermal noise n_t , then $N_0/A^2 = 2b_L/\rho = -84$ dB, which is the standalone value of $S_\phi(0)$ ($=S_\phi(10)$). In effect, this pertains to the 1420-MHz signal. According to Eq. (2), the receiver value of $S_\phi(0)$, which pertains to a 100-MHz signal, is $(14.2)^2 = 23$ dB below the standalone value. Allan deviation can be obtained (Ref. 6) by

$$\sigma_y(\tau) = \frac{\sqrt{3S_\phi(0)b_L}}{2\pi f_0 \tau} \quad (\text{A-1})$$

$$= \frac{8.7 \times 10^{-14}}{\tau}$$

Front end (module A). The noise n_A is amplifier phase jitter, as opposed to additive thermal noise. The figures for $\Delta f/f$ and $S_\phi(10)$ are merely requirements from Ref. 1. Amplifiers are observed to exhibit flicker phase modulation (Ref. 7), which means that $S_\phi(f) = \text{const}/f$ for $0 < f < f_h$, where f_h is a cutoff frequency, set to 100 Hz here. The Allan deviation is then equal to

$$\sigma_y(\tau) = \frac{2.42 \sqrt{S_\phi(10)}}{f_0 \tau} \sqrt{1 + 0.13 \ln \tau} \quad (\text{A-2})$$

(Ref. 6, corrected in a memorandum of D. W. Allan.)

First IF (module B), second IF (module C), phase detector (module D). Same remarks as for module A. The $\Delta f/f$ and $S_\phi(10)$ values are requirements from Ref. 1, and flicker PM is assumed.

$\times 14$ multiplier (module M). The $\Delta f/f$ value is from Ref. 8. Reference 9 gives $S_\phi(f) = 10^{-10}/f$ for $1 \leq f \leq 100$ Hz. The receiver value is 23 dB lower. Equation (A-2) gives $\sigma_y(\tau)$.

Dana synthesizer (module G). The $\Delta f/f$ is scaled from the value given in Ref. 10 for a 25°C step. To get the receiver value, multiply by 0.4/1420. The $S_\phi(10)$ value is scaled from

the value given in Ref. 11 for a Dana synthesizer at 40 MHz instead of 0.4 MHz. Since this is also flicker PM, Eq. (A-2) gives $\sigma_y(\tau)$.

VCO (module E). The VCO phase noise appears outside the one-sided loop passband (50 Hz). We assume it to be pure flicker frequency modulation, $S_\phi(f) = c/f^3$, such that for all τ of interest, $\sigma_y(\tau) = 2 \times 10^{-12}$, the requirement from Ref. 1. This number appears under $\Delta f/f$ in Table 1, although it has nothing to do with a temperature step. From Ref. 6 we can deduce $c = f_0^2 \sigma_y^2 / \ln 4$, where $f_0 = 100$ MHz, and thence the standalone $S_\phi(10)$. Since 10 Hz is well within the loop passband, we have not attempted to compute the receiver $S_\phi(10)$. To obtain the receiver $\sigma_y(1)$, one realizes that the VCO phase noise, highpass filtered by the loop, is stationary, with variance approximately equal to

$$\sigma_E^2 = \int_{50}^{\infty} \frac{c}{f^3} df = 5.8 \times 10^{-12}$$

One can then use Eq. (A-1) to get $\sigma_y(\tau)$ by substituting σ_E^2 for $S_\phi(0)b_L$.

100-MHz distribution amplifier (module F). Let us first remark that the contribution of this amplifier to all outputs (multiplied to 100 MHz) is about

$$- \frac{14}{14.2} n_{F7} + n_{Fi}$$

where $i = 13, 8$, or 19 . This is why the receiver values of $\Delta f/f$ and $S_\phi(10)$ are double the standalone values. Reference 12 gives a phase change $0.08 \text{ deg}/^\circ\text{C}$ at 10 MHz; this scales to $\Delta\phi = 4 \text{ deg}$ at 100 MHz for a 5°C change. Following R. Meyer's advice, we computed

$$\frac{\Delta f}{f} = \frac{2}{3} \frac{\Delta\phi}{2\pi f_0 \tau} \quad (\text{A-3})$$

with $f_0 = 100$ MHz, $\tau = 2000$ s. The idea is that the phase response to the temperature step has a time constant about 2000 s. This is a rough estimate, of course. For $S_\phi(f)$ we use

the measurements of Meyer and Sward (Ref. 7), which, scaled to 100 MHz, give $S_{\phi}(f) = 8 \times 10^{-11}/f$. Equation (A-2) gives $\sigma_y(\tau)$.

Divider – cleanup filter – DA (modules H-L). The performance breakdown of these combinations is given in Table 2,

which, as usual, assumes that the output has been multiplied to 100 MHz. Flicker PM is assumed for all components. Sources are Refs. 7 and 13 for the divider, Ref. 14 for the cleanup filter, and Refs. 7 and 12 for the DA. There are two receiver entries in Table 1 for the 20-MHz module *H* because this module feeds backward into the loop and also forward into its own output.

References

1. Meyer, R. F., "Hydrogen Maser Frequency Standard: Receiver Configuration and Stability Requirements," *The Deep Space Network Progress Report*, Technical Report 32-1526, Vol XVIII, pp. 66-72. Jet Propulsion Laboratory, Pasadena, Calif., December 15, 1973.
2. Finnie, C., Sydnor, R., and Sward, A., "Hydrogen Maser Frequency Standard," *Proceedings of the 25th Annual Frequency Control Symposium*, pp. 348-351. U.S. Army Electronics Command, Fort Monmouth, New Jersey, April 28, 1971.
3. Sward, A., "Measurement of the Power Spectral Density of Phase of the Hydrogen Maser," *JPL Quarterly Technical Review*, Vol. I, Number 4, pp. 30-33. Jet Propulsion Laboratory, Pasadena, Calif., January 1972.
4. Kuhnle, P. F., "Hydrogen Maser Implementation in the Deep Space Network at the Jet Propulsion Laboratory," Proc. 11th Annual PTTI Applications & Planning Meeting, Goddard Space Flight Center, Greenbelt, Md., Nov. 1979.
5. Greenhall, C. A., "Removal of Drift from Frequency Stability Measurements," *TDA Progress Report 42-65*, Jet Propulsion Laboratory, Pasadena, Calif., 1981.
6. Barnes, J. A., et al., Characterization of Frequency Stability, NBS Technical Note 394, National Bureau of Standards, Washington, D.C., 1970.
7. Meyer, R., and Sward, A., "Frequency Generation and Control: The Measurement of Phase Jitter," *The Deep Space Network, Space Programs Summary 37-64*, Vol. II, pp. 55-58. Jet Propulsion Laboratory, Pasadena, Calif., August 31, 1970.
8. MacConnell, J., Meyer, R., "L-Band Frequency Multipliers: Phase Noise, Stability, and Group Delay," *The Deep Space Network Progress Report*, Technical Report 32-1526, Vol. X, pp. 104-109. Jet Propulsion Laboratory, Pasadena, Calif., August 15, 1972.
9. Lutes, G., MacConnell, J., and Meyer, R., "Hydrogen Maser: Low Phase Noise, L-Band Frequency Multiplier," *The Deep Space Network Progress Report*, Technical Report 32-1526, Vol. VII, pp. 81-83. Jet Propulsion Laboratory, Pasadena, Calif., February 15, 1972.
10. Sward, A., "New Developments in the Hydrogen Maser Frequency Standard," *The Deep Space Network Progress Report*, Technical Report 32-1526, Vol. II, pp. 72-74. Jet Propulsion Laboratory, Pasadena, Calif., April 15, 1971.
11. Greenhall, C. A., Internal Noise of a Phase-Locked Receiver with a Loop-Controlled Synthesizer, *DSN Progress Report 42-52*, pp. 41-50, Jet Propulsion Laboratory, Pasadena, Calif., 1979.
12. Lutes, G., "Frequency Generation and Control: Distribution Amplifiers for the Hydrogen Maser Frequency Standard," *The Deep Space Network, Space Programs Summary 37-61*, Vol. II, pp. 68-72. Jet Propulsion Laboratory, Pasadena, Calif., January 31, 1970.
13. Lutes, G., "Improved Frequency Dividers," *The Deep Space Network Progress Report*, Technical Report 32-1526, Vol. II, pp. 56-58. Jet Propulsion Laboratory, Pasadena, Calif., April 15, 1971.
14. Lutes, G. F., "Phase-Stable, Low-Phase-Noise Filters for Reference Signals," *The Deep Space Network Progress Report*, Technical Report 32-1526, Vol. XII, pp. 44-46. Jet Propulsion Laboratory, Pasadena, Calif., December 15, 1972.